Flexural characteristics of rubberized cement-stabilized crushed aggregate for pavement structure

Ahmed Hilal Farhan*[1, 2], Andrew Robert Dawson[1], Nicholas Howard Thom[1], Sarhat Adam[1], Martin John Smith[1]

Accepted manuscript

http://dx.doi.org/10.1016/j.matdes.2015.09.071

Please cite this article as: A.H. Farhan, et al., Flexural characteristics of rubberized cement-stabilized crushed aggregate for pavement structure, Materials and Design (2015), http://dx.doi.org/10.1016/j.matdes.2015.09.071

Flexural characteristics of rubberized cement-stabilized crushed aggregate for pavement structure

Ahmed Hilal Farhan*[1, 2], Andrew Robert Dawson[1], Nicholas Howard Thom[1], Sarhat Adam[1], Martin John Smith[1]

[1] School of Civil Engineering, Faculty of Engineering, University of Nottingham, University Park, Nottingham NG7 2RD, UK, Tel: +44 (0) 7448461314, E-mail: evxahfa@nottingham.ac.uk

[2] Civil Engineering Department, College of Engineering, Al-Anbar University, Iraq

*corresponding author

Abstract

The purpose of this paper is to investigate the flexural characteristics and to quantitatively study the flexural-induced cracking of reference and rubberized cement stabilized aggregate mixtures. Four volumetric replacement percentages (0%, 15%, 30% and 45%) of 6 mm fraction size were used. This modification was found to affect the material strength detrimentally. However, material toughness was improved and stiffness was reduced. The latter findings were supported by quantitative assessment of the fractured surfaces which revealed more tortuous and rougher cracking as a result of rubber content increasing. This, in turn, may ensure a good load transfer across the cracks after their formation. Overall, using rubber in pavement construction is a sustainable solution that ensures consumption of large quantities of these waste materials. At the same time, it may considered as a promising method to reduce cracking tendency and sensitivity which may improve shrinkage, thermal and fatigue performance.

Keywords: cement stabilized aggregate; rubberized cement stabilized mixture; flexural behaviour; fractured surface characterization; ultrasonic testing

1. Introduction

The increased number of tyres stockpiled every year has created a serious economic and environmental problem. Disposal sites may become places for breeding of creatures that spread many diseases and can cause significant fire hazard (Zheng et al. 2008). Consequently, to deal with these problems and to save natural resources, many studies (Khatib and Bayomy 1999; Güneyisi et al. 2004; Papakonstantinou and Tobolski 2006; Balaha et al. 2007; Zheng et al. 2007; Khaloo et al. 2008; Taha et al. 2008; Zheng et al. 2008; Topçu and Bilir 2009; Nguyen et al. 2010; Pelisser et al. 2011; Najim and Hall 2012; Eiras et al. 2014) have been conducted to investigate the properties of rubberized concrete. How feasible is it to use waste tyres in concrete structure by replacing the fine, coarse or fine and coarse aggregate with rubber particles of different sizes and shapes? In general, the above researchers' findings revealed that replacing natural aggregate with rubber particles decreased the strength, although some researchers (Jingfu et al. 2009) reported a slight increase in tensile strength. However, less stiffness, less brittleness and improvement in toughness was obtained as results of aggregate replacement by coarse or fine rubber particles (Balaha et al. 2007; Taha et al. 2008).

In pavement structures, it is customarily to use cement stabilized aggregate as a base or subbase course to increase the structural capacity of that structure, namely in terms of strength and stiffness. Cement stabilized aggregate (CSA) is a mixture of aggregate, cement and a small amount of water (Lim and Zollinger 2003). Unlike normal concrete, cement stabilized aggregate contains a low amount of cement and is constructed by rolling. In spite of the similarity between cement stabilized aggregate and roller compacted concrete in terms of construction method, the latter usually contains cement contents approaching that used in normal concrete (PCA 2005) .

Different testing methods are used to characterize the stabilized aggregate mixtures. These include uniaxial compressive testing (Lim and Zollinger 2003), direct tensile testing (Shahid 1997), indirect tensile testing (Hudson and Kennedy 1968; Khattak and Alrashidi 2006) and flexural testing (Disfani et al. 2014; Arulrajah et al. 2015). The tensile properties in terms of flexural strength and indirect tensile are considered critical for pavement design (Xuan et al. 2012). However, the flexural testing mode is most preferable test (Arulrajah et al. 2015) used since it is the most simulative to what actually happening in the field (Arnold et al. 2012). In the Mechanistic- Empirical (M-E) pavement design guide, CSA layers are usually designed to resist tensile fatigue failure at the bottom of that layer. This requires estimation of flexural strength as an important parameter. Therefore, reduction of stiffness without significant strength loss, which rubber addition might achieve, could be an attractive option as it would be likely to reduce the applied stress and, hence, extend fatigue life.

A very limited number of studies have been conducted regarding the effect of rubber on the behaviour of cement stabilized aggregate intended to be used for pavement structure (Guo et al. 2013). Since the construction of highways consumes large quantities of natural resources as compared with other engineering applications, using crumb rubber in this application is a highly sustainable option (Cao 2007; Barišić et al. 2014). Furthermore, it may mitigate the disadvantages of cement stabilization regarding high stiffness and brittleness. Another motivation comes from the fact that since the mix will be compacted, this might ensure a good interaction between the rubber and the natural aggregate particles as compared with wet-cast concrete mixtures. For the above reasons, the purpose of this paper is to study the effect of crumb rubber on the flexural properties of rubberized cement stabilized aggregate (R-CSA).

2. Experimental Program

2.1 Properties of materials used

The aggregate used in this study is a crushed limestone, with a nominal maximum size of 20 mm, obtained from Dene quarry in Nottinghamshire, UK. This was collected in different sizes (20mm, 14mm, 10mm, 6mm and dust (< 6mm)). These were dried then the gradation for each fraction size was estimated by sieve analysis in accordance with BS EN 933-1:2012. The crumb rubber (Figure 1) was sourced from J Allcock and Sons Ltd. in Manchester, UK. Its gradation is presented in Figure 2. Two reasons are behind selecting this size. Firstly, from the economic point of view, this size is cheaper and commonly available as compared with finer ones (Najim 2012). Secondly, initial examination showed that the gradation of this size is similar to that of the 6 mm natural aggregate fraction (Figure 2) which would be likely to enable replacement of some of the latter size without a big change in volumetric relationships of the mix. Hence its use would permit estimation of the effect of rubber replacement alone. The specific gravity of the rubber was adopted as a 1.12 as measured by (Najim and Hall 2012). An Ordinary Portland cement CEM I 52.5 R conforming to BS EN 197-1: 2000 was used as the binding agent. Potable tap water is used across this investigation.

2.2 Mixture design

To constitute the required Cement bound granular mixture (CBGM) gradation as stated in BS EN 14227-1:2013- [CBGM2-0/20] , all five aggregate fractions sizes were combined together in different proportions using the trial and error method (Garber and Hoel 2009). These proportions are 11%, 20%, 11%, 13% and 45% for 20mm, 14mm, 10mm, 6mm and dust, respectively. The final gradation after blending all sizes in these proportions is illustrated in Figure 3. The cement content used to stabilize the aggregate mixture was 5% of the dry weight of aggregate. Optimum water content as a percentage of the dry weight of cement and aggregate was estimated through the compactibility test in accordance with BS EN 13286-4:2003. This was done by constructing a water content-maximum density relationship as presented in Figure 4. Since the gradations of 6 mm natural aggregate and crumb rubber are similar, it was decided to replace the former by the latter volumetrically to help ensure the same packing. Thus, investigate the effect of aggregate type. Three volumetric replacement percentages were taken into considerations. These are 15%, 30% and 45% of the 6 mm aggregate fraction volume, which are equivalent to 2.1%, 4.2% and 6.2% of the total volume of the aggregate, respectively. To produce comparable mixtures, the quantity of water and cement was kept constant for all replacement levels. Conventionally (and for the reference mix) water and cement contents were computed as percentages of the dry weight of aggregate in the conventional mix. As rubber replacement would change this weight due to its low specific gravity, mix design maintained the same volumetric proportions and hence the same opportunities for packing of aggregate with the same surrounding mortar. Table 1 shows the investigated mixtures which are designated as follows: C5R0 for the reference mixture without rubber whereas C5R15, C5R30 and C5R45 are used to describe the mixtures containing 15%, 30% and 45% rubber replacement, respectively.

2.3 Mixing and sample preparation

All mixing was conducted in a pan mixture with a capacity of 0.1 m^3. In terms of mixing sequence, the cement and dust were firstly mixed together until a uniform colour was achieved then this was added to the rest of aggregate and mixed thoroughly for one minute. After that, mixing for another two minutes was done after adding the required quantity of water. A standard 100 mm x 100 mm x 500 mm steel mould was used for manufacturing prisms. In order to achieve a uniform density, regular dimensions and a smooth surface for accurate testing, a mould extension was fabricated to fit on top of the mould and used so that more than a 100 mm height was achieved. The specimen was then sawn down to 100 mm height. After placement in the mould, the mixture was compacted in three layers using a Kango 368 vibrating hammer fitted with a 100 mm x 100 mm square tamper. The compaction time was 60 second per layer and each was scarified prior to compacting the next layer.

Triplicate samples were manufactured for each mix. All manufactured samples were left inside their moulds and covered with wet paper and polythene sheets to prevent moisture loss. After 24 hours, they were demoulded and wrapped with nylon film and placed in wet polythene bags and closed tightly. Then, they were moved to the humid room and kept for 28 days.

2.4 Testing procedures

Flexural testing was conducted in accordance with BS 188: Part 118:1983. A 200 KN capacity closed loop deflection controlled Zwick 1484 universal testing machine was used for the static flexural testing program. Four point bending test configuration was used for prismatic specimens spanning 300 mm. To obtain the post-peak load-deflection behaviour, the test was conducted under deformation control at a stroke rate of 0.05 mm/min and corresponding deflection was measured at mid-span of beams using two linear variable differential transducers (LVDTs). These were mounted utilizing a yoke arrangement. The average value from these two LVDTs was used as a deflection at each load application. Figure 5 illustrates the flexural testing configuration.

The ultrasonic pulse velocity (UPV) and dynamic modulus of elasticity were measured non-destructively in accordance with ASTM C597 using the PUNDIT- plus apparatus. This was done by measuring the stress wave speed by the direct transmission method from transducer to receiver. Then, from the measured UPVs values, the dynamic modulus of elasticity (E_d) was also calculated as follows (Mardani-Aghabaglou et al. 2013):

$$Ed = \frac{\rho\, \mathrm{UPV}^2 (1+\nu)(1-2\nu)}{1-\nu}$$

where ρ and ν are the density and Poisson`s ratio, respectively. The bulk density of the fabricated beams was estimated using the water displacement method.

3. Results and discussion

3.1 Bulk density and rubber distribution

Table 1 shows the effect of rubber substitution on the bulk density of test samples. It can be clearly seen that, as expected, replacement of natural aggregate with crumb rubber causes a decrease in the bulk density since the specific gravity of rubber particles is much lower than that of natural aggregate. This can also be attributed to the higher elasticity of rubber particles which might have a detrimental effect on the effectiveness of the compaction. The rate of decrease in density was about 16 Kg/m^3 for every 1% increase in rubber content which is consistent with the findings of Khatib and Bayomy (1999) who investigated the replacement with rubber (albeit in conventional concrete) of fines-only, only-coarse fraction and of both fine and coarse fractions.

Regarding the rubber distribution, Figure 6 illustrates the rubber distribution (at mid height of the sample) for different investigated mixtures. For C5R30 mix, rubber distribution is shown at three levels of the prism height (top, mid, and bottom). As shown in the latter figure, a uniform rubber distribution was achieved for all replacements. Unlike the normal wet-cast concrete mixtures where the rubber may float upwards due to the vibration as well as the consistency of this mixture, compacted CSA with relative dry consistency shows a fairly uniform rubber distribution across the individual levels. This, in turn, might ensure a uniform stress distribution inside the mixture since, otherwise, the accumulation of rubber due to non-uniform distribution might cause stress concentrations and accelerate sample failure accordingly.

3.2 Flexural properties

3.2.1 Flexural strength

Tests were conducted at 28-day age and triplicate specimens were used for each mix. The flexural strength was computed utilizing the formula $F_s = PL/bh^2$where Fs, L, P, b, h are the flexural strength, span, ultimate load, width of the prism and height of the prism, respectively. Figure 7 illustrates the effect of rubber replacement on flexural strength. A clear reduction in strength is seen as the amount of replacement increases. It seems that the introduction of rubber has an adverse effect on the aggregate interlocking, which can be considered, in this type of mixture, as the main factor for frictional resistance development. The latter is the mechanism by which the compacted mixtures resist applied traffic loading. In addition, the reduction in flexural strength can be attributed also to the drop in both tensile and compressive strengths due to replacement of natural aggregate of high strength by the softer rubber particles.

3.2.2 Flexural stiffness

Flexural stiffness as reported by (Turatsinze and Garros 2008) can be calculated as a slope ($\Delta P/\Delta\delta$) of the linear part of load-deflection curve based on the 30% pf the ultimate load and its corresponding deflection (Arnold et al. 2012) . Figure 7 clearly shows that there was a reduction in stiffness of the mixture as a result of rubber replacement. This can be attributed to the lower modulus of elasticity of the rubber particles. This confirms previous findings for concrete mixtures (Turatsinze and Garros 2008; Najim and Hall 2012).

3.2.3 Flexural toughness

Toughness can be considered as an indication of the ability of material to absorb energy (Erdem 2012) or, in other words, it is an expression of the energy required to fail the specimen. Regarding normal concrete, a limited number of researches have been conducted to quantify the toughening effect due to rubber replacement (Najim and Hall 2012). Toughness was estimated from the area under the load-deflection curves (Figure 8) based on the ASTM C 1018 method which is most widely used. This specification defines the toughness in terms of three indices (I_5, I_{10} and I_{20}) which were calculated by dividing the area under the load-deflection curve at deflections of 3, 5.5 or 10 times the first crack deflection, respectively, by the area under the curve up to the deflection when the first crack was observed.

The conclusion that can be drawn from Figure 9 is that the replacement of natural aggregate by rubber enhances the toughness of the resulted mixtures. This might be partly because rubber particles contribute to delay the micro-crack initiation by stress relaxation (Najim and Hall 2012) and/or due to lengthening of the crack path by propagation through the rubber particles. Many authors (Toutanji 1996; Aiello and Leuzzi 2010; Guleria and Dutta 2011; Najim 2012) have reported similar improvement in toughness due to the inclusion of rubber in concrete mixtures. In addition, this means improvement in deformability of material and, hence, the formation of a more ductile material (Topcu 1995). In fact, this may ensure a mixture with less sensitivity to fatigue cracking which is, as reported by (Brown 2012), the main mode of failure in bound base courses of pavement structures. The investigation of fatigue characteristics has been undertaken but will be presented in a separate paper.

3.3 Ultrasonic pulse velocity and dynamic modulus of elasticity

Figure 10 shows the relative dynamic modulus of elasticity and ultrasonic pulse velocity (UPV) of rubberized mixtures with respect to the reference one. This figure revealed that a decrease in wave velocity by 3.6%, 4.7% and 7.9% occurred when the 6 mm fraction aggregate was replaced by 15%, 30% and 45% crumb rubber particles, respectively. There was also a commensurate decrease in the compacted dynamic modulus of elasticity values by 7.7%, 10.65% and 18.5%. These changes may be because of the interlocking of rubber particles with natural aggregate causing loss of contact points between stiff aggregate particles which in turn would affect the transmission of ultrasonic wave. In addition, the lower modulus of elasticity of the rubber particles relative to that of the conventional aggregate may explain the reductions. Similarly, in concrete technology, where the UPV and dynamic modulus of elasticity is frequently used for assessing concrete quality non-destructively, many authors (Zheng et al. 2008; Najim and Hall 2012) have reported similar behaviour for rubberized normal concrete.

Figure 11 shows that the flexural strength is fairly well correlated with the UPVs. One application of this relationship is the possibility to estimate the flexural strength (and hence the stress ratio) for the flexural fatigue test. Mechanistic pavement design is significantly dependent on the fatigue performance of the bound mixtures, and the stress ratio at which they are called to operate plays a crucial role. Stress ratio can be defined as the ratio between the applied flexural stress and strength. In the latter test, the conventional approach is to measure the flexural strength of the mixture based on the static flexural test then to estimate the stress ratios to be applied to the different specimens in flexural fatigue tests. However, due to the heterogeneity of CSA, this approach does not necessarily ensure that a representative flexural strength is obtained. (Sobhan and Das 2007) tried to overcome this by correlating the flexural strength of full-sized beams to the flexural and compressive strengths of beams and cubes sawn from fatigue failed specimens. In this way they were able to estimate the actual flexural strength and, hence, stress ratio of the fatigued specimens. In this paper, the suggested correlation between flexural strength and UPV provides a means of better estimating the flexural strength, non-destructively, for the same specimen to be used for the fatigue test instead of totally relying on estimation of this parameter based on static flexural testing. This methodology may also help to reduce the cost and time of specimen sawing and testing.

4 Quantification of the flexural induced cracks

To provide more understanding regarding the effect of rubber on the behaviour of CSA and the mechanism of its failure, a quantitative evaluation of the flexural induced fractured surfaces was performed in terms of surface tortuosity and volumetric surface texture ratio (VSTR). Tortuosity can be defined as the ratio between the actual crack length and the projection of that crack (Hassan 2012). In this paper, the earlier definition was extended to evaluate the 3D tortuosity as the ratio of the surface area of the fractured surface to the projection of that surface. The surface area was calculated according to the methodology presented in (Chupanit and Roesler 2008). The VSTR is the surface parameter that can be calculated from the volume between the actual surface and the mean plane of the surface as shown below (Chupanit and Roesler 2008)

$$\mathrm{VSTR} = \frac{\sum |R_i \ A_i| + \sum |S_j A_j|}{\sum (A_i + A_j)}$$

where R_i=distance above the mean plane; S_j= distance below the mean plane; A_i or A_j = projected area of each small element (1 mm^2).To estimate above surface parameters, it necessary to acquire the fractured surface in terms of xyz coordinates to use them in surface creation. This was done utilizing the photogrammetry procedure

4.1 Photogrammetric procedure

It is well known that many methods are available for characterizing and modelling 3D surfaces, for example, laser scanning or photogrammetry. There are two main approaches that can be used to process digital images to generate 3D surfaces using either algorithms from photogrammetry or the structure from motion (SfM) technique which has been largely developed by the computer vision community. Using close range photogrammetry, it is possible to reach an estimated accuracy of better than 1mm with non-metric cameras (Remondino and Fraser 2006). There are a number of commercial photogrammetric software packages accurate 3D surface measurements. In SfM however, often the visualisation and automation of 3D model is more important than the accuracy. Similar to stereo-photogrammetry, SfM can use a set of images acquired with a consumer grade camera to generate a 3D surface. The main difference compared to photogrammetry is that image acquisition can be more flexible in relative position and attitude of the images. The procedures that both photogrammetry and SfM share are; camera calibration, image matching, and inverse triangulation with bundle adjustment for 3D point cloud generation. Figure 12 shows this sequence of activities.

The photogrammetric and SfM processes were used to generate the 3D surface modelling of fractured concrete samples in terms of a cloud of X, Y, Z coordinated points. To minimize the processing time and to help extraction of the coordinates defining the fractured surface, the sides of each sample were painted white and placed on a white background. This helped the process of removing unwanted point as it is easier to differentiate points on the fractured surface from those on the white surfaces. A datum is required to define the coordinate system and four specially designed markers of 0.5x0.5 cm were placed on each of the samples as shown in Figure 13 and surveyed using a reflectorless total station in order to produce coordinates so they could be used as control points in the image orientation process, see Figure 12.

Eight fractured samples were modelled and transformed to their ‘total station' coordinate system utilizing the aligning tool in Cloud Compare (CC), (CloudCompare 2013) . Cloud compare provides details of the transformation process such as the transformation matrix, RMSE of the transformation and the recovered scale. With 4 control points on each sample the RMSE values of the residuals give a quality estimate of transforming each sample to local ‘total station’ coordinate system This gives an indication of the estimated quality of the coordinates defining the surface. RMSE values for different scanning are tabulated in Table 2. As can see from the latter table, significant differences among RMSE values exist between different samples of the same mixture especially for C5R0 and C5R15. This can be attributed to the process of surveying and measuring targets or the difference in the angle of image capturing during image acquisition process, where the RMSEs is a scanning-dependent parameter. However, as can be seen from Table 2 all the Root Mean Square Error (RMSE) values are well below 1mm with an average RMSE value of 0.64mm. This was considered acceptable for the purposes of these experiments. Based on the work by Beshr and Abo Elnaga (2011), RMSE values of less than 0.2mm are achievable for the coordinates of the marks based on a range of less than 2m, and an inclination of less than 45°, so there appears to be the possibility of further improving the technique in the future.

4.2 Fractured surface quantification findings

Based on the above procedure the 3D digital fractured surfaces were constructed from the xyz coordinates for each surface as shown Figure 14. From these surfaces, the tortuosity and VSTR were estimated as mentioned earlier. Figure 15 reveals that the inclusion of rubber causes greater tortuosity and VSTR for all replacement levels. This can be explained as follows. An increase in the embedded rubber particles increases the number of weak points because of the large differences between moduli of rubber and adjacent particles. This, in turn, may causes cracks to divert via these weak points, hence changing (and may be lengthening) the crack path so that it becomes more tortuous. However, amongst the rubberized mixtures, the smaller differences between the value of both VSTR and tortuosity might be because the local distribution of the crumb rubber inside the sample. In addition, each surface parameter gave different ranking where C5R15 has the larger VSTR while C5R30 has the larger tortuosity. (Chupanit and Roesler 2008) have reported the same behaviour and they attributed that to unavoidable differences in the scale and resolution when scanning to assess both surface parameters. The practical implication of tortuosity increase means production of tougher and less brittle materials as observed by (Guo et al. 2007) who introduced a brittleness parameter as the inverse of the tortuosity value (brittleness parameter $=A/A_s$, where A_s and A represent the surface area of the fracture surface and the projection of that surface, respectively). The rougher crack is likely to ensure good load transfer efficiency across the crack after its formation (Vandenbossche 1999; Vandenbossche et al. 2014) from which greater material toughness results.

In support of the above hypothesis that the rubber deflects the crack route through the mixture, the amount of rubber per perpendicular unit length across the fractured surface was determined by an image processing technique utilizing the ImageJ software. Firstly, the fracture surfaces images were captured using a high resolution camera. Then these were converted from RGB mode to an 8 bytes greyscale. ImageJ tools were then utilized to conduct thresholding (Figure 16) and eventually estimation of the rubber content across this surface. The resulting measurement was compared with the quantity used which was known from the mix design. It was found, as shown in Figure 17, that the quantity of rubber visible on the crack surface is more than that used. Furthermore, this difference increases as rubber content increases. The above results confirm that the cracks propagate around rubber particles which support the conjecture of longer crack paths. This explanation is further supported by the measured toughness index changes.

5. Conclusions

In this paper, the effect of rubber replacement on the properties of cement stabilized aggregate with emphasis on flexural properties was investigated. In the light of the findings the following conclusions can be drawn:

1. Flexural strength, density and stiffness were reduced as a result of rubber replacement. However, more ductile mixtures were produced as confirmed by toughness improvement. This was further confirmed by ultrasonic testing where both dynamic modulus of elasticity and UPV decreased due to the introduction of rubber particles. This indicates that both the studied mixture and normal concrete exhibit similar trends of behaviour when rubber is added.

2. Quantitative assessment of the fractured surfaces revealed that as the rubber replacement level increased, the tortuosity and the VSTR of the crack surfaces increased. This means more fracture energy was dissipated. These, combined with an evaluation of the rubber content on fractured surfaces, may lead to an improved understanding of the mechanism of the failure.

3. A good correlation was found between flexural strength and UPV values. This may enable accurate estimation of the static flexural strength of the material non-destructively. This in turn will help to overcome problems associated with the heterogeneity of this type of cementitious mixture when performing fatigue tests.

4. Use of the crumb rubber in compacted cement stabilized mixtures aggregate does not experience the same segregation difficulties as encountered in conventional concrete after casting and vibration.

5. In spite the decline in the flexural strength of the mixtures due to rubber incorporation, the use of rubber will be justified since this detrimental impact on the flexural strength may be balanced by the other advantages like improvement in the cracking pattern (achieving good load transfer across the crack) and ,importantly, disposing of the waste materials. Furthermore, reduction in stiffness will reduce the stress experienced at the bottom of the stabilized layer.

6. More investigation is required to assess the performance of rubberized cement stabilized mixtures in terms of fatigue performance and durability so as to evaluate and validate their use.

Acknowledgements

The support from Higher Committee of Education Development in Iraq (HCED) by providing a scholarship for this research is gratefully acknowledged. Thanks are also due to Dr. Luis Neves for his valuable advices.

Figure Captions

Fig.1. Appearance of rubber used in this study.

Fig.2. Individual grain size distribution of the 6 mm fraction size and rubber.

Fig.3 Mixture gradation after blending all different sizes.

Fig.4 Water content- dry density relationship.

Fig.5 Flexural test configuration.

Fig.6 Distribution of rubber for different replacement levels: (a) C5R15-mid (b) C5R30-top (c) C5R30-middle (d) C5R30-bottom (e) C5R45-mid.

Fig.7. Effect of rubber replacement on flexural strength and stiffness.

Fig.8. Load-deflection curves for investigated mixtures.

Fig.9. Effect of rubber replacement on toughness indices.

Fig.10. Ultrasonic dynamic moduli and UPVs for different mixtures.

Fig.11 Relationship between UPV and flexural strength.

Fig.12. A flow diagram of the photogrammetric and structure from motion processes.

Fig.13. Fixing markers on the fractured surfaces.

Fig.14. Samples of fractured surfaces scan: a. C5R0, b. C5R30.

Fig.15. VSTR and tortuosity of investigated mixtures.

Fig.16. Analysis of rubber quantity through fractures surface: a. captured image, b. thresholded image and c. thresholding process.

Fig.17. Effect of replacement level on amount of rubber across the fractured surfaces.

Table 1: Investigated mixtures details and designation

Mixture	Cement content(% by wt. of aggregate and cement of control mix)	Rubber content(%by volume of 6mm fraction size)	Water (% wt. of aggregate and cement of control mix)	Bulk Density Kg/m^3
C5R0	5	0	4.6	2529.647 (0.1%)
C5R15	5	15	4.6	2494.5 (0.17%)
C5R30	5	30	4.6	2456.433 (0.2%)
C5R45	5	45	4.6	2418.533 (0.24%)

Values in the brackets are the coefficient of variation.

Table2: RMSE of the residuals at the control points on the fractured surface

Sample ID	C5R0-1	C5R0-2	C5R15-1	C5R15-2	C5R30-1	C5R30-2	C5R45-1	C5R45-2
RMSE (mm)	0.54	0.20	0.68	0.44	0.84	0.82	0.88	0.73

Figure 1: Appearance of rubber used in this study.

Figure 2: Individual grain size distribution of the 6 mm fraction size and rubber

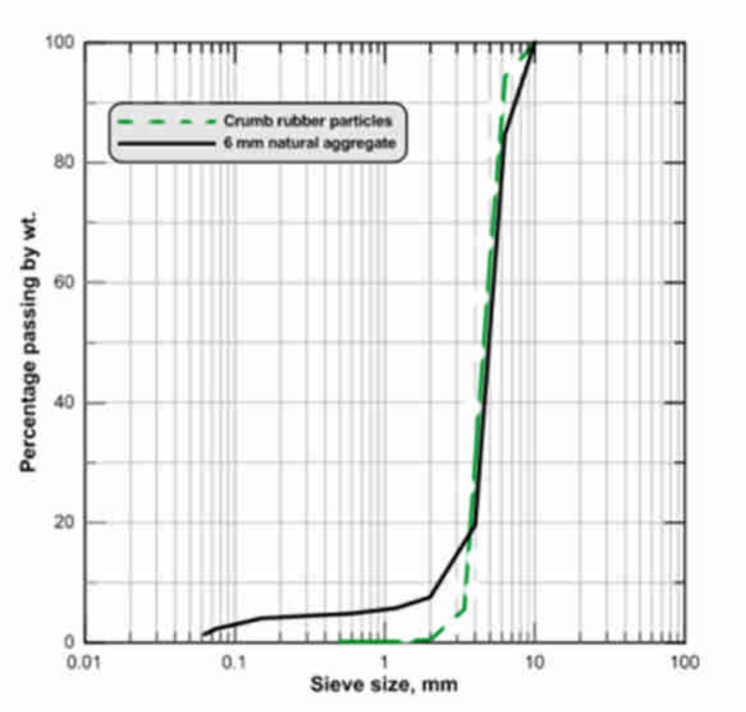

Figure 3: Mixture gradation after blending all different aggregate sizes.

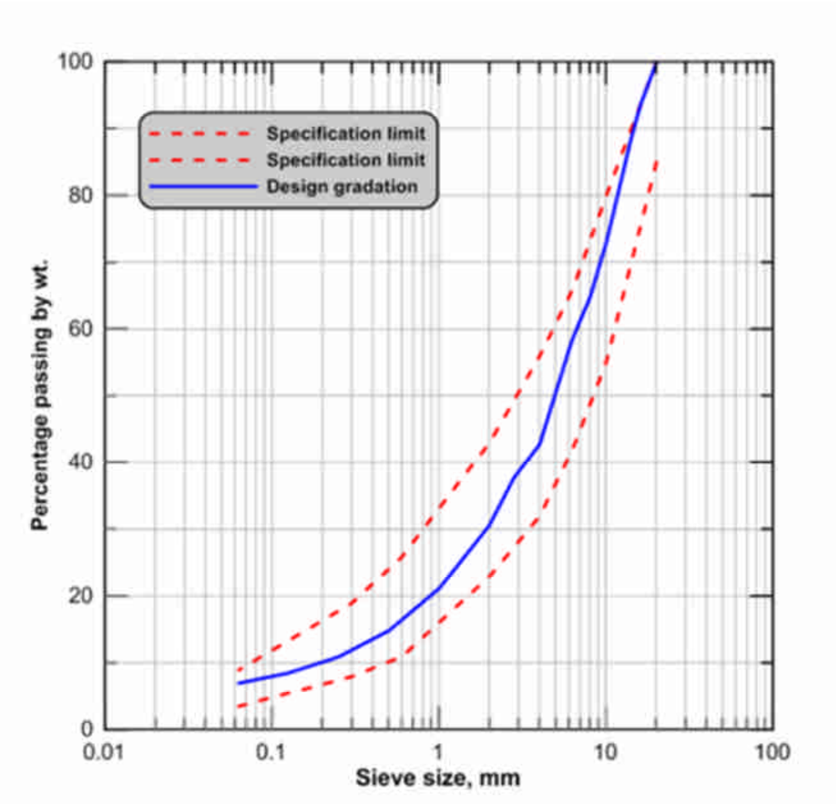

Figure 4: Water content- dry density relationship.

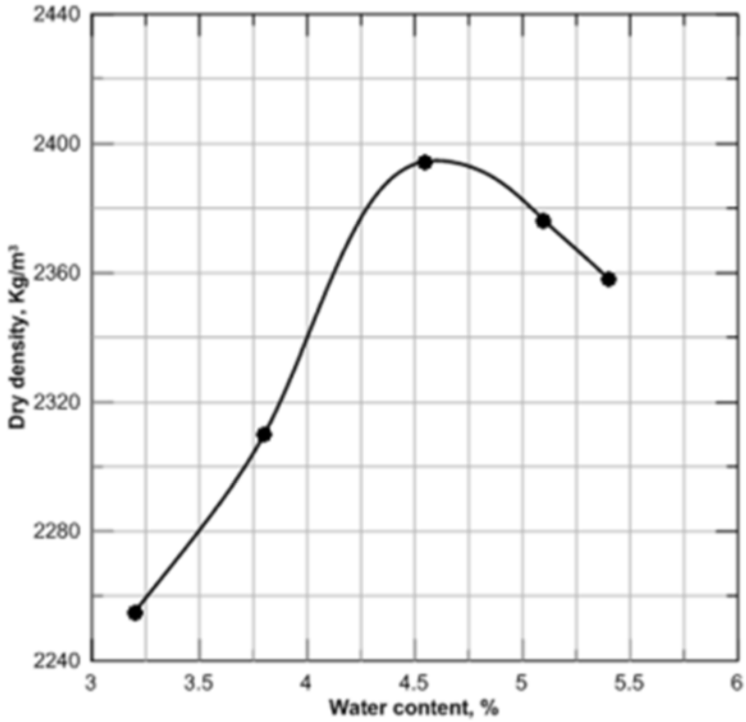

Figure 5: Flexural test configuration

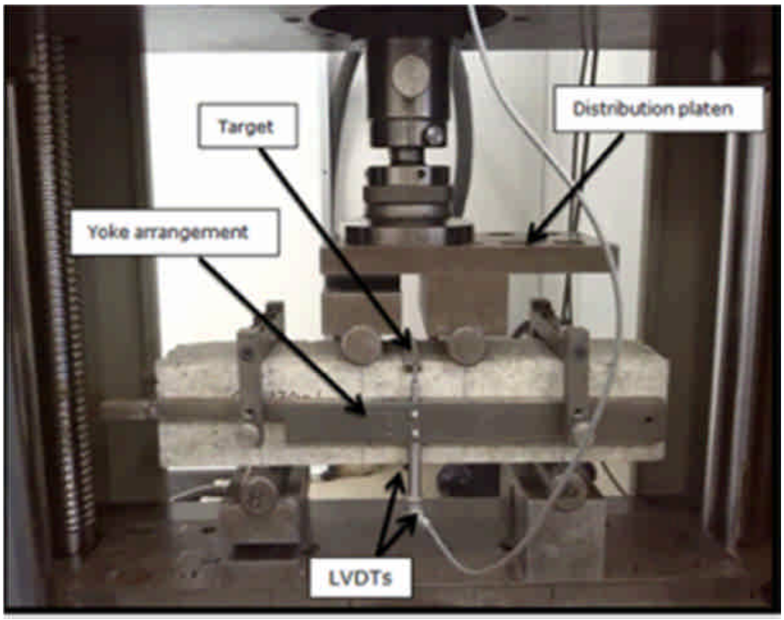

Figure 6: Distribution of rubber for different replacement levels: (a) C5R15-mid (b) C5R30-top (c) C5R30-middle (d) C5R30-bottom (e) C5R45-mid

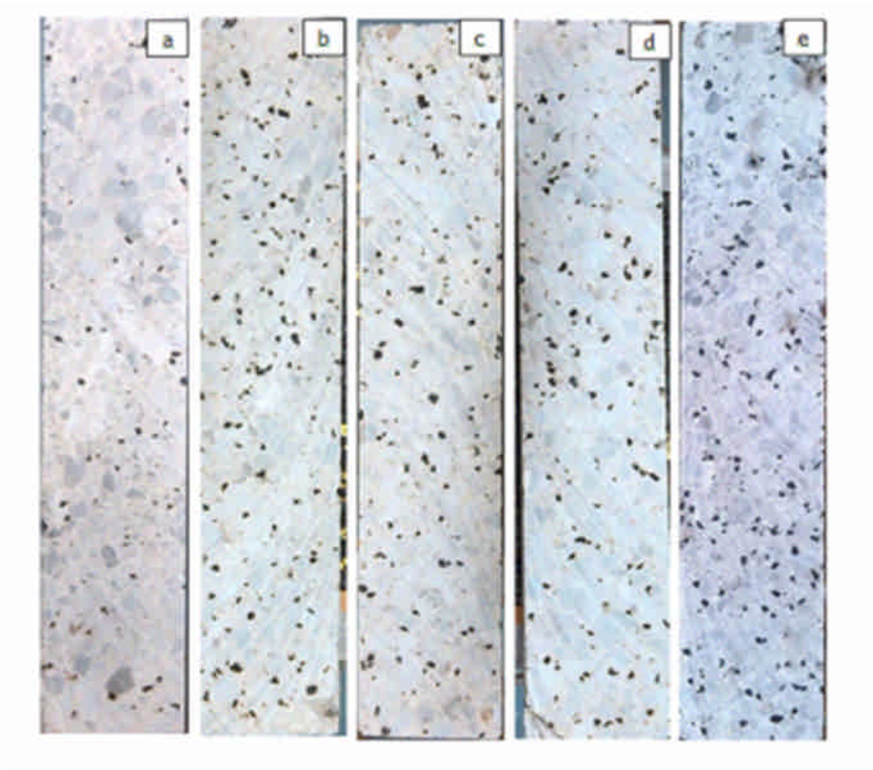

Figure 7: Effect of rubber replacement on flexural strength and stiffness

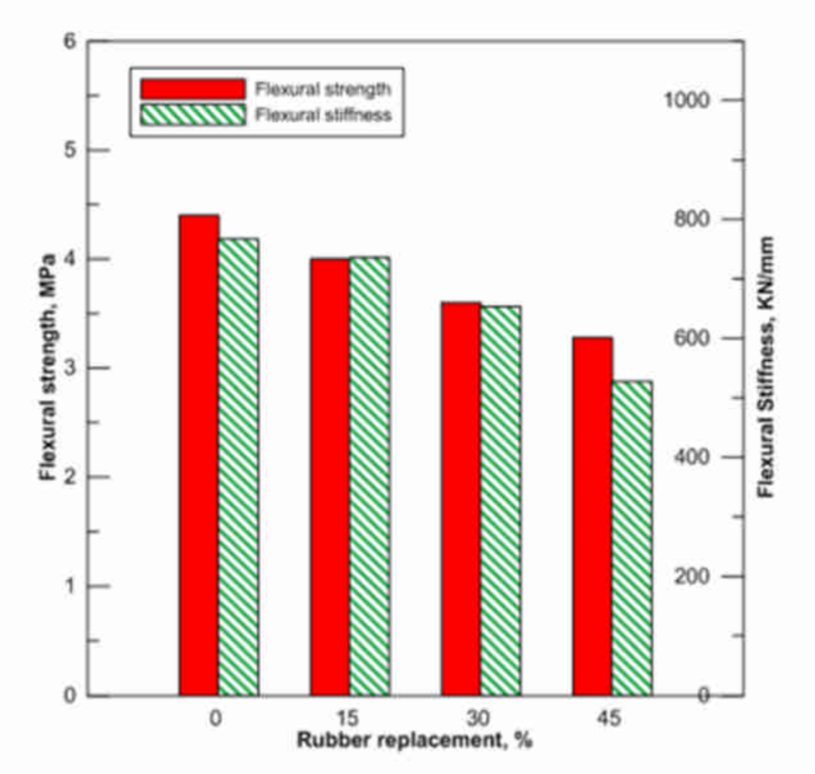

Figure 8: Load-deflection curves for investigated mixtures.

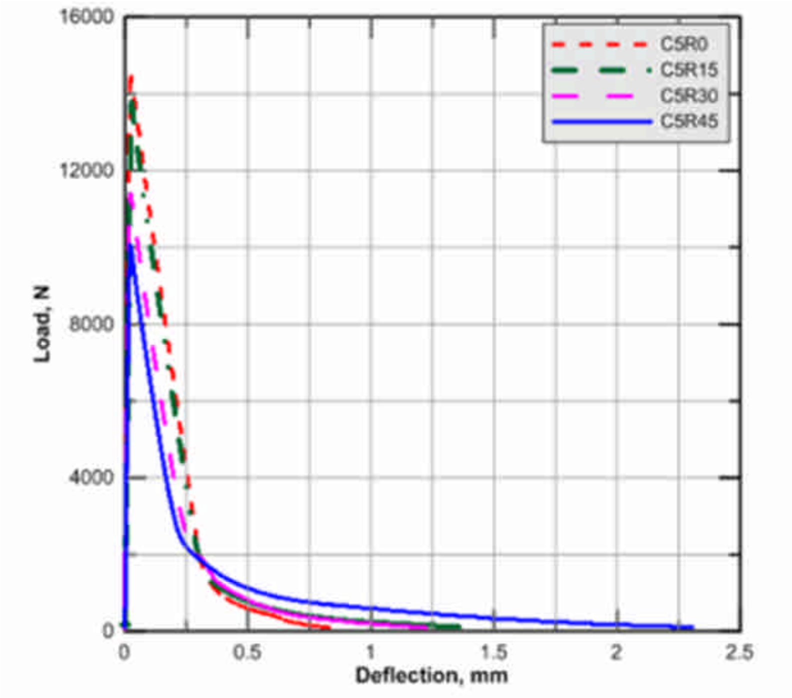

Figure 9: Effect of rubber replacement on toughness indices

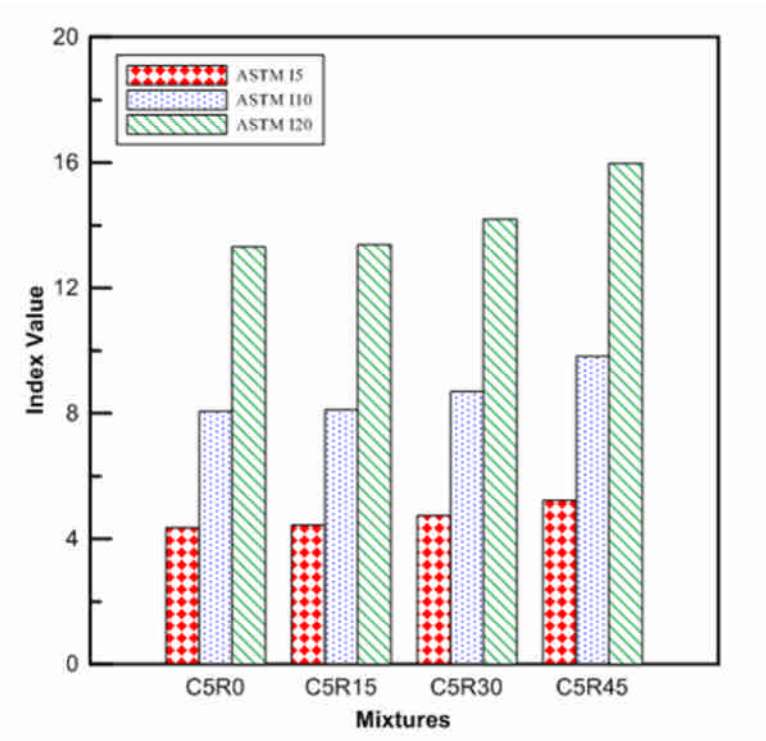

Figure 10: Ultrasonic dynamic moduli and UPVs for different mixtures

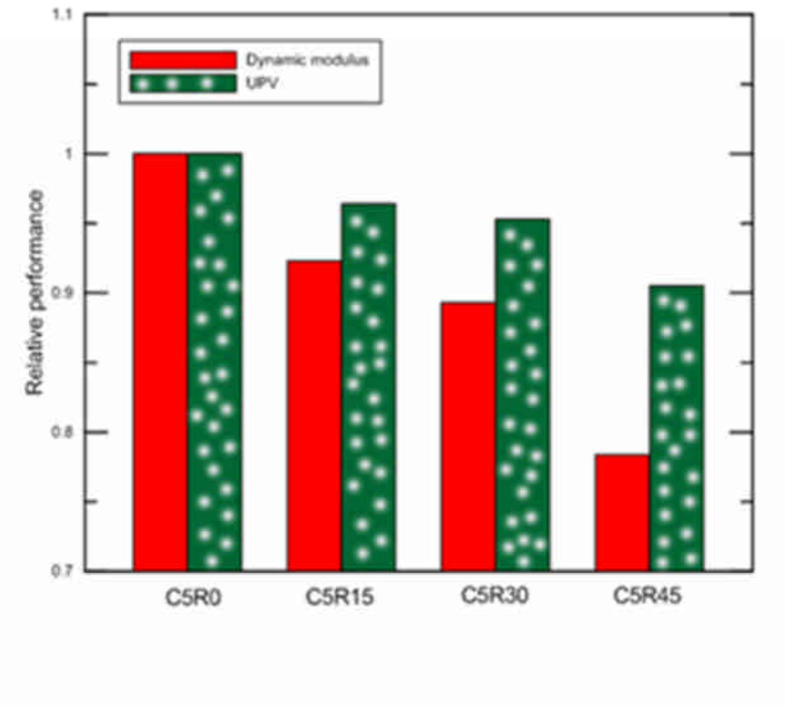

Figure 11: Relationship between UPV and flexural strength.

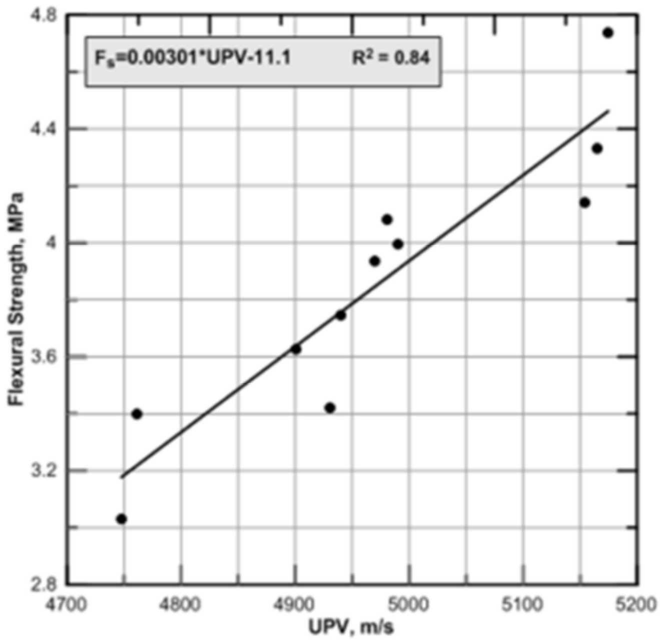

Figure 12 A flow diagram of the photogrammetric and structure from motion processes.

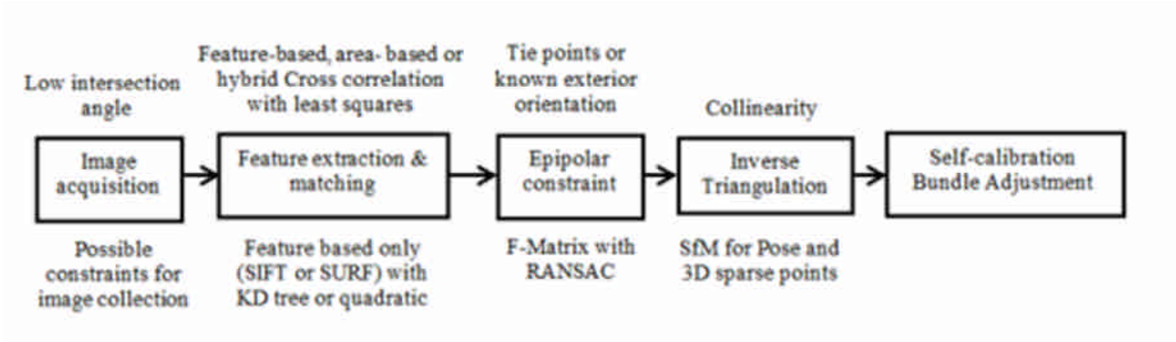

Figure 13: Fixing markers on the fractured surfaces.

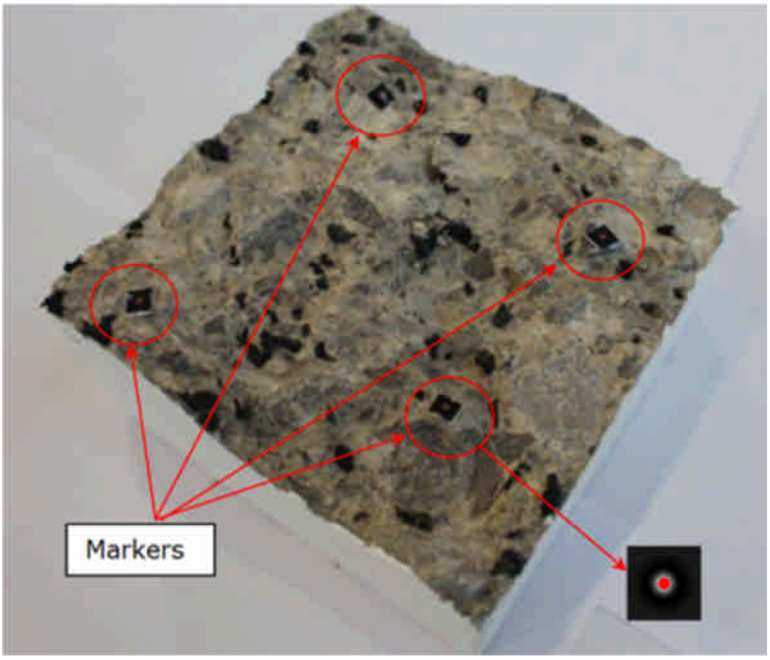

Figure 14: Samples of fractured surfaces scan: a. C5R0, b. C5R30

(a)

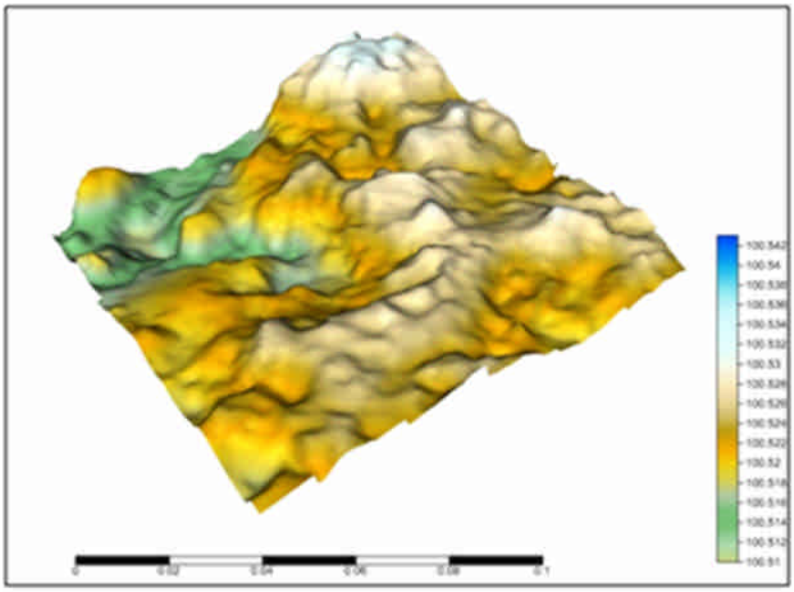

(b)

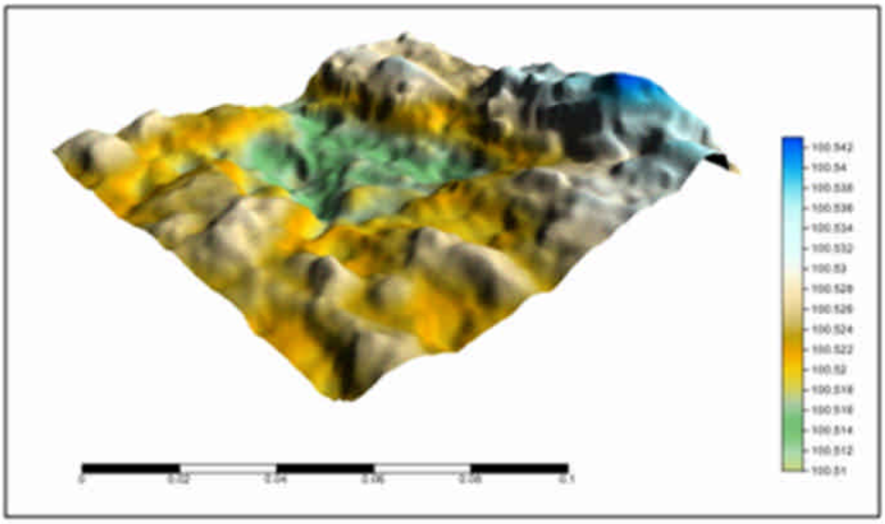
100.542
100.54
100.538
100.536
100.534
100.532
100.53
100.528
100.526
100.524
100.522
100.52
100.518
100.516
100.514
100.512
100.51

Figure 15: VSTR and tortuosity of investigated mixtures

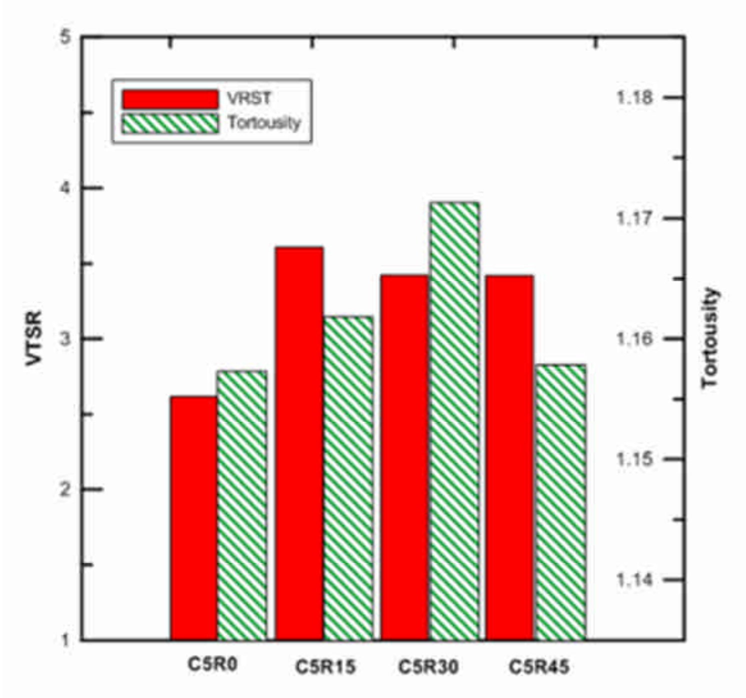

Figure 16: Analysis of rubber quantity through fractures surface: a. captured image, b. thresholded image and c. thresholding process

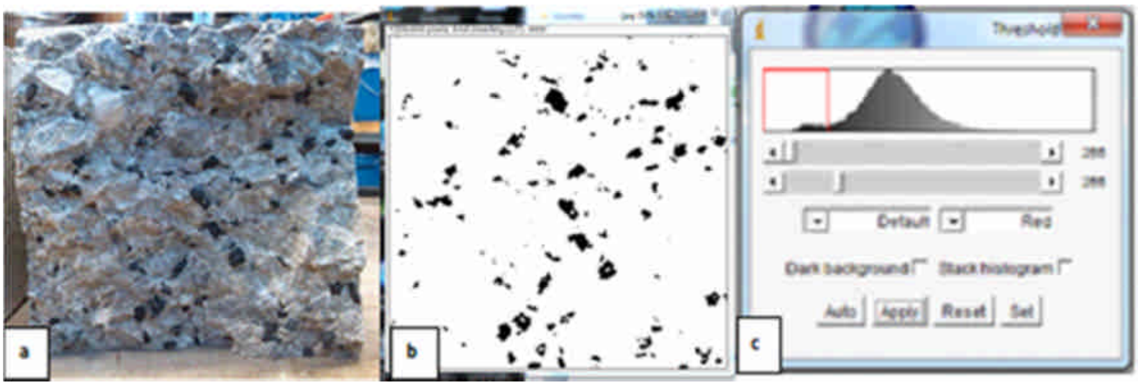

Figure 17: Effect of replacement level on amount of rubber across the fractured surfaces.

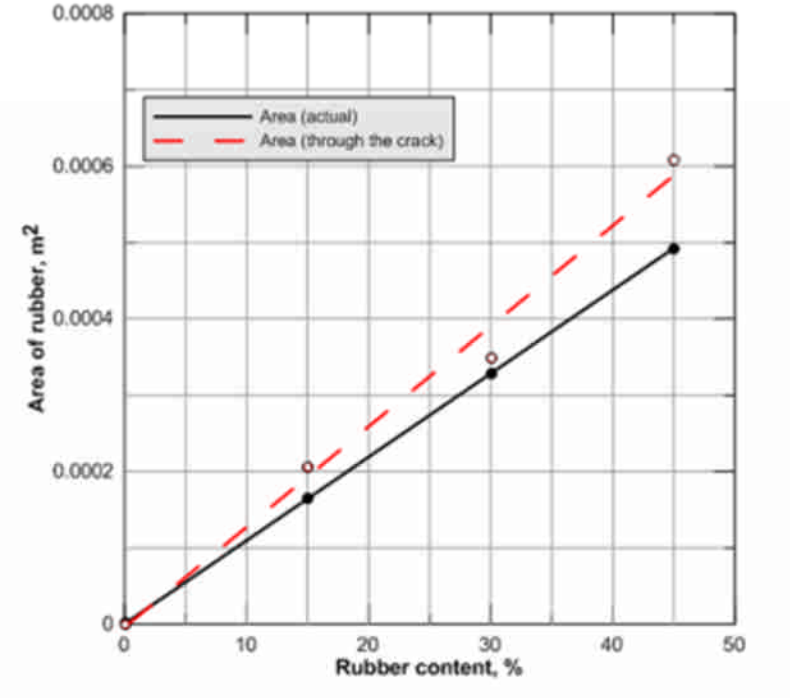

References

Aiello, M. A. and F. Leuzzi (2010). "Waste tyre rubberized concrete: properties at fresh and hardened state." Waste Manag **30**(8-9): 1696-1704.

Arnold, G., C. Morkel, et al. (2012). Development of tensile fatigue criteria for bound materials.

Arulrajah, A., M. M. Disfani, et al. (2015). "Modulus of rupture evaluation of cement stabilized recycled glass/recycled concrete aggregate blends." Construction and Building Materials **84**: 146-155.

Balaha, M. M., A. A. M. Badawy, et al. (2007). "effect of using ground waste tire rubber on the behavior of concrete mixes." Indian journal of Engineering and Materials Science **14**: 427-435.

Barišić, I., S. Dimter, et al. (2014). "Strength properties of steel slag stabilized mixes." Composites Part B: Engineering **58**: 386-391.

Beshr, A. A. A. and I. M. Abo Elnaga (2011). "Investigating the accuracy of digital levels and reflectorless total stations for purposes of geodetic engineering." Alexandria Engineering Journal **50**(4): 399-405.

Brown, S. F. (2012). "An introduction to asphalt pavement design in the UK." Proceedings of the ICE-Transport **166**(4): 189-202.

Cao, W. (2007). "Study on properties of recycled tire rubber modified asphalt mixtures using dry process." Construction and Building Materials **21**(5): 1011-1015.

Chupanit, P. and J. R. Roesler (2008). "Fracture energy approach to characterize concrete crack surface roughness and shear stiffness." Journal of Materials in Civil Engineering **20**(4): 275-282.

CloudCompare (2013). 3D point cloud and mesh processing software

Open Source Project, EDF.

Disfani, M. M., A. Arulrajah, et al. (2014). "Flexural beam fatigue strength evaluation of crushed brick as a supplementary material in cement stabilized recycled concrete aggregates." Construction and Building Materials **68**: 667-676.

Eiras, J., F. Segovia, et al. (2014). "Physical and mechanical properties of foamed Portland cement composite containing crumb rubber from worn tires." Materials & Design **59**: 550-557.

Erdem, S. (2012). Impact load-induced microstructural damage of concrete made with unconventional aggregates. PhD thesis, University of Nottingham.

Garber, N. J. and L. A. Hoel (2009). Traffic & highway engineering, Cengage Learning.

Guleria, S. and R. Dutta (2011). "Unconfined compressive strength of fly ash–lime–gypsum composite mixed with treated tire chips." Journal of Materials in Civil Engineering **23**(8): 1255-1263.

Güneyisi, E., M. Gesoğlu, et al. (2004). "Properties of rubberized concretes containing silica fume." Cement and Concrete Research **34**(12): 2309-2317.

Guo, H. M., H. Zhu, et al. (2013). "The Applied Research of Waste Crumb Rubber in Road Base." Applied Mechanics and Materials **253**: 317-321.

Guo, L.-P., W. Sun, et al. (2007). "Study on the flexural fatigue performance and fractal mechanism of concrete with high proportions of ground granulated blast-furnace slag." Cement and Concrete Research **37**(2): 242-250.

Hassan, N. A. (2012). Microstructural characterization of rubber modified asphalt mixtures PhD, The university of Nottingham.

Hudson, W. R. and T. W. Kennedy (1968). An indirect tensile test for stabilized materials, Center for Highway Research, University of Texas at Austin.

Jingfu, K., H. Chuncui, et al. (2009). "Strength and shrinkage behaviors of roller-compacted concrete with rubber additives." Materials and Structures **42**(8): 1117-1124.

Khaloo, A. R., M. Dehestani, et al. (2008). "Mechanical properties of concrete containing a high volume of tire-rubber particles." Waste Management **28**(12): 2472-2482.

Khatib, Z. K. and F. M. Bayomy (1999). "Rubberized Portland cement concrete." Journals of Materials in Civil Engineering, ASCE **11**: 206-213.

Khattak, M. J. and M. Alrashidi (2006). "Durability and mechanistic characteristics of fiber reinforced soil–cement mixtures." International Journal of Pavement Engineering **7**(1): 53-62.

Lim, S. and D. G. Zollinger (2003). "Estimation of the compressive strength and modulus of elasticity of cement-treated aggregate base materials." Transportation Research Record: Journal of the Transportation Research Board **1837**(1): 30-38.

Mardani-Aghabaglou, A., Ö. Andiç-Çakir, et al. (2013). "Freeze–thaw resistance and transport properties of high-volume fly ash roller compacted concrete designed by maximum density method." Cement and Concrete Composites **37**: 259-266.

Najim, K. B. (2012). Determination and enhancement of mechanical and thermo-physical behaviour of crumb rubber-modified structural concrete. PhD thesis, The University of Nottingham.

Najim, K. B. and M. R. Hall (2012). "Mechanical and dynamic properties of self-compacting crumb rubber modified concrete." Construction and Building Materials **27**(1): 521-530.

Nguyen, T., A. Toumi, et al. (2010). "Mechanical properties of steel fibre reinforced and rubberised cement-based mortars." Materials & Design **31**(1): 641-647.

Papakonstantinou, C. G. and M. J. Tobolski (2006). "Use of waste tire steel beads in Portland cement concrete." Cement and Concrete Research **36**(9): 1686-1691.

PCA (2005). "soil cement technology for pavement different products for different applications." Portland Concrete Association(illinois).

Pelisser, F., N. Zavarise, et al. (2011). "Concrete made with recycled tire rubber: Effect of alkaline activation and silica fume addition." Journal of Cleaner Production **19**(6-7): 757-763.

Remondino, F. and C. Fraser (2006). "Digital camera calibration methods: considerations and comparisons." International Archives of Photogrammetry, Remote Sensing and Spatial Information Sciences **36**(5): 266-272.

Shahid, M. A. (1997). "Improved Cement Bound Base Design for Flexible Composite Pavement." PhD Thesis, University of Nottingham.

Sobhan, K. and B. M. Das (2007). "Durability of soil–cements against fatigue fracture." Journal of Materials in Civil Engineering **19**(1): 26-32.

Taha, M. M. R., A. S. El-Dieb, et al. (2008). "Mechanical, Fracture, and Microstructural Investigations of Rubber Concrete." Jounal of Materials in Civil Engineering, ASCE **20**: 640-649.

Topcu, I. B. (1995). "The properties of rubberized concrete." Cement and Concrete Research **25**(2): 304-310.

Topçu, İ. B. and T. Bilir (2009). "Experimental investigation of some fresh and hardened properties of rubberized self-compacting concrete." Materials & Design **30**(8): 3056-3065.

Toutanji, H. A. (1996). "The Use of Rubber Tire Particles in Concrete to Replace Mineral Aggregates." Cement & Concrete Composkes **18**: 135-139.

Turatsinze, A. and M. Garros (2008). "On the modulus of elasticity and strain capacity of self-compacting concrete incorporating rubber aggregates." Resources, conservation and recycling **52**(10): 1209-1215.

Vandenbossche, J. M. (1999). "Estimating potential aggregate interlock load transfer based on measurements of volumetric surface texture of fracture plane." Transportation Research Record: Journal of the Transportation Research Board **1673**(1): 59-63.

Vandenbossche, J. M., M. Barman, et al. (2014). "Using Surface Texture Measurements of a Crack Surface to Establish a Joint Spring Stiffness Representing the Shear Transfer Capacity." Transportation Research Record: Journal of the Transportation Research Board.

Xuan, D., L. Houben, et al. (2012). "Mechanical properties of cement-treated aggregate material–a review." Materials & Design **33**: 496-502.

Zheng, L., X. Sharon Huo, et al. (2007). "Experimental investigation on dynamic properties of rubberized concrete." Construction and Building Materials **22**(5): 939-947.

Zheng, L., X. Sharon Huo, et al. (2008). "Strength, Modulus of Elasticity, and Brittleness Index of Rubberized Concrete." Journal of Civil Engineering , ASCE.